

## **FUSE OBSERVATIONS OF THE CYGNUS LOOP: PROBING SHOCK-CLOUD INTERACTIONS**

R. Sankrit and W. P. Blair

The Johns Hopkins University, Baltimore, USA

### RESUMEN

Presentamos observaciones hechas con el satélite *FUSE* de la emisión de O VI  $\lambda\lambda$  1032, 1038 proveniente de los choques no radiativos y radiativos en el remanente de supernova del *Rizo del Cisne*. Se pueden utilizar los perfiles de velocidad de las líneas y la variación espacial de sus flujos para estudiar la distribución de los componentes emisores y la geometría de los choques. El cociente entre los flujos de los dos componentes puede ser utilizado para evaluar los efectos de tanto la dispersión por resonancia como la absorción por material a lo largo de la visual. La emisión de O VI varía sistemáticamente con la emisión de H $\alpha$  detrás de los choques no radiativos suaves pero las dos tienen distribuciones muy diferentes en las regiones complejas de interacción entre los choques y las nubes. La emisión de O VI traza el gas que tiene temperatura del orden de 300,000 K, es decir, más caliente que los filamentos ópticos y más frío que las regiones que emiten rayos-X, y por lo tanto nos proporciona un diagnóstico muy importante para los estudios a multifrecuencias de los choques de remanentes de supernova.

### ABSTRACT

We present *FUSE* observations of O VI  $\lambda\lambda$  1032, 1038 emission from non-radiative and radiative shocks in the Cygnus Loop supernova remnant. The velocity profiles of the lines and the spatial variation of their fluxes can be used to study the distribution of the emitting components and the shock geometry. The ratio between the fluxes of the two components can be used to evaluate the effects of both resonance scattering and absorption by material along the line of sight. The O VI emission varies systematically with the H $\alpha$  behind smooth non-radiative shocks but the two are distributed very differently in complex shock-cloud interactions. O VI traces gas at about 300,000 K, hotter than the optical filaments and cooler than the X-ray regions, and thus provides a crucial diagnostic for multi-wavelength studies of SNR shocks.

**Key Words:** ISM: INDIVIDUAL (CYGNUS LOOP) — ISM: SHOCKS — SUPERNOVA REMNANTS

### 1. INTRODUCTION

The emission from the Cygnus Loop supernova remnant (SNR), in all passbands from the radio to the X-ray, is dominated by shocks running into interstellar clouds that lie around its perimeter. Among the strongest lines emitted by these shocks are O VI  $\lambda\lambda$  1032, 1038. Observations of the Cygnus Loop using *Voyager 1* and *2* (Blair et al. 1991b; Vancura et al. 1993) and the rocket-borne HIREs (Rasmussen & Martin 1992) show that O VI emission is an important channel through which the remnant loses energy. These studies show that the O VI luminosity of the Cygnus Loop is roughly the same as its luminosity in the 0.1–4.0 keV X-ray band, the latter based on *Einstein* observations (Ku et al. 1984). Spectra of the Cygnus Loop obtained with the *Hopkins Ultraviolet Telescope* (*HUT*) show that a copious amount of O VI emission is produced both in radiative shocks (Blair et al. 1991a) and non-radiative shocks (Long et al. 1992) with velocities  $\gtrsim 170 \text{ km s}^{-1}$ .

We have used the *Far Ultraviolet Spectroscopic Explorer* (*FUSE*) to measure the O VI emission at several locations in the Cygnus Loop. *FUSE* is an excellent instrument for such a study because of its high spectral resolution and its sensitivity to diffuse emission. The line profiles are resolved in our spectra, and the spatial distribution of the O VI emission is mapped on sub-arcminute and arcminute scales by suitable choices of aperture locations. The observations presented here are a subset of those of the Cygnus Loop obtained as part of a PI team project. Details of the observations are given by Sankrit & Blair (2002) and Blair, Sankrit, & Tulin (2002).

### 2. A NON-RADIATIVE SHOCK

A set of five observations was obtained with the MDRS ( $4'' \times 20''$ ) aperture sampling the structure across a Balmer filament in the northeast Cygnus Loop. The filament traces a  $170 \text{ km s}^{-1}$  non-radiative shock front running into a cloud which has

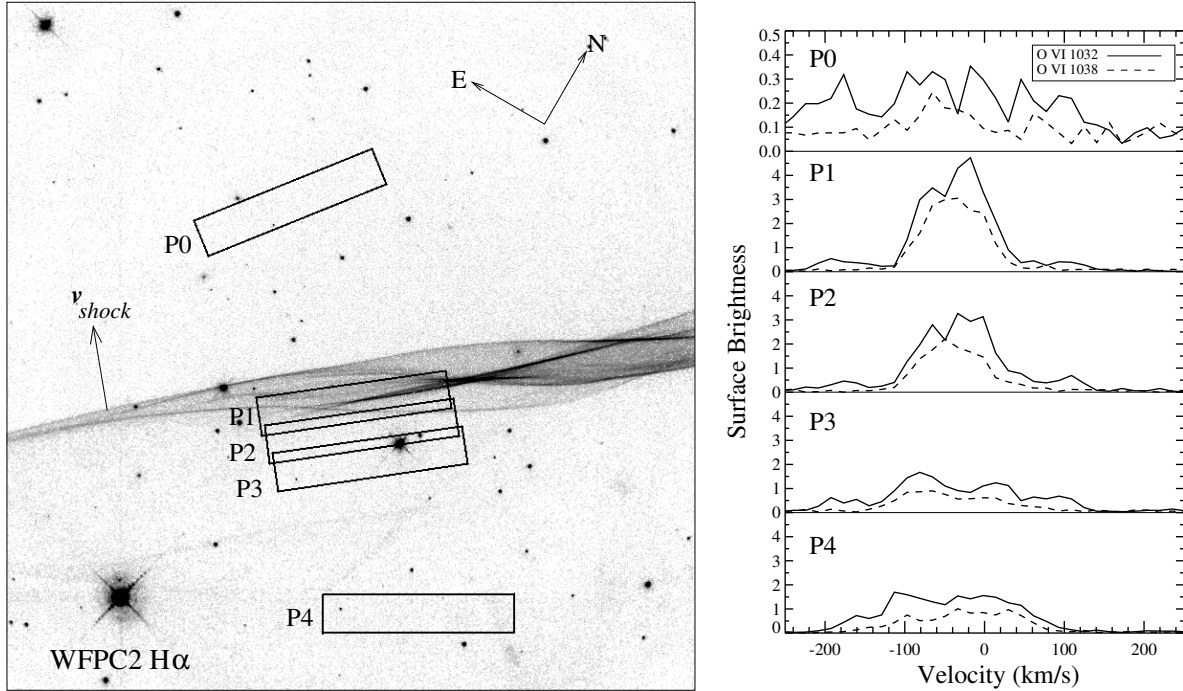


Fig. 1. Left panel: WFPC2  $H\alpha$  image of a non-radiative filament in the northeast Cygnus Loop, overlaid with *FUSE* MDRS aperture locations. The boxes are  $20'' \times 4''$ . Right panel: O VI  $\lambda\lambda$  1032, 1038 surface brightness profiles (the units are  $10^{-15} \text{ erg s}^{-1} \text{ cm}^{-2} \text{ arcsec}^{-2} \text{ \AA}^{-2}$ ) plotted against the local-standard-of-rest velocity. Note the vertical scale in the top panel (P0): though not obvious in this representation, a fit to the background shows that O VI emission is detected.

a density of about  $3 \text{ cm}^{-3}$  (Long et al. 1992; Hester, Raymond, & Blair 1994; Sankrit et al. 2000). In Figure 1, (left) the MDRS aperture positions are shown overlaid on a WFPC2  $H\alpha$  image (Blair et al. 1999). The O VI surface brightnesses are plotted on the right. The spectra show that the O VI surface brightness follows the  $H\alpha$  closely through positions 1, 2, and 3. The O VI at position 0 is fainter than at the other positions by at least an order of magnitude and is probably associated with the faster blast wave that in projection is beyond the Balmer filament. At position 4, the flux is about the same as at position 3. However, there are faint Balmer filaments near position 4, which indicate the presence of other non-radiative shocks in the region. At positions 1, 2, and 3, there are fainter components on the blue and red wings of the 1032  $\text{\AA}$  line that are symmetrically placed about the center and they have the same intensity at all three positions. In the context of the cavity model (Levenson et al. 1998) the wing emission components may arise in the neutral shell that covers a large fraction of the surface of the remnant.

### 3. SHOCKED RADIATIVE CLOUD

*FUSE* MDRS spectra were obtained at two nearby locations on a bright cloud on the Eastern

limb of the Cygnus Loop. The spacecraft was oriented so that the HIRS ( $1''.25 \times 20''$ ) and LWRS ( $30'' \times 30''$ ) apertures lay on different parts of the shocked region. The  $H\alpha$  image of the field, with four of the aperture positions overlaid, is shown in Figure 2 (left). The spectra sample regions with different morphologies and a range of  $H\alpha$  brightnesses. The O VI surface brightnesses are shown in Fig. 2 (right). The strongest emission is from the bright  $H\alpha$  knot (E1 MDRS position) but the emission from the HIRS positions are not much weaker, even though there is little  $H\alpha$ . The O VI surface brightness in the LWRS spectrum is lower still, even though it lies on an  $H\alpha$  knot. The O VI emission is more widely distributed than the optical emission, and arises in both radiative and non-radiative shocks.

In Figure 3, the E1 MDRS spectrum O VI 1032  $\text{\AA}$  and 1038  $\text{\AA}$  line fluxes, and their ratio are plotted against velocity. The ratio near the line center is close to 1, implying that the emission is optically thick. Towards the wings the ratio rises and approaches 2, which is expected if the line is optically thin. At velocities below  $-100 \text{ km s}^{-1}$  and at around  $+100 \text{ km s}^{-1}$  the ratio is higher than 2 because the wings of the 1038  $\text{\AA}$  line have been absorbed by overlying molecular hydrogen along the line of sight.

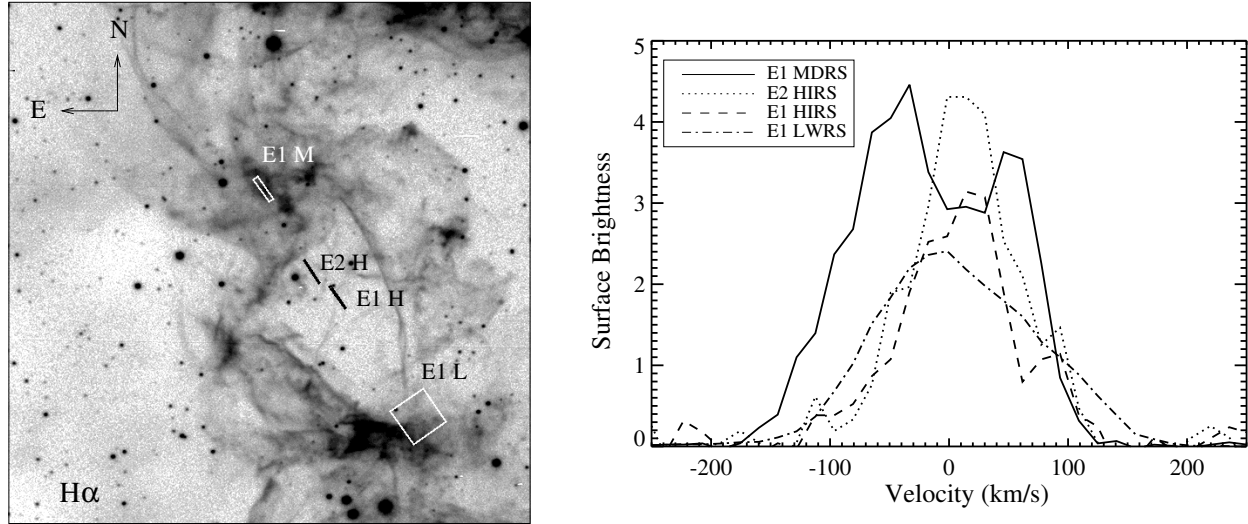


Fig. 2. Left panel: H $\alpha$  image overlaid with a subset of the *FUSE* aperture locations through which spectra were obtained. The boxes are drawn to scale; the LWRS aperture is 30'' on the side. Right panel: O VI  $\lambda$ 1032 surface brightness profiles (units as in Fig. 1) at the four locations plotted against velocity. The peak O VI brightness varies little though the H $\alpha$  changes dramatically.

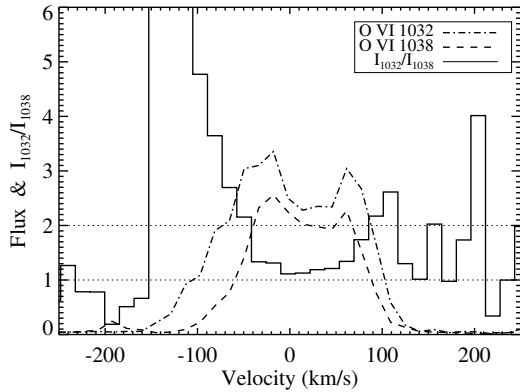


Fig. 3. E1 MDRS spectrum: O VI line fluxes and ratio between them.

#### 4. CONCLUDING REMARKS

The spatial distribution of O VI emission, its correlation with the H $\alpha$  and with the X-ray emission, and the velocity structure of the lines are useful data for understanding the nature of SNR shocks. In the case of non-radiative filaments (§ 2; see also Raymond 2003) the observations can be interpreted in a relatively straightforward way since the geometry is simple and the O VI emission varies systematically behind the shock front. However, in the case of the shock-cloud interaction on the eastern limb (§ 3) the morphology of the emission is complex, and instabilities in the flow may contribute to the velocity structure. Currently, multi-dimensional hydro-

dynamic models of shock interactions do not include the full range of atomic physics needed for realistic line-flux predictions. These, and other *FUSE* observations of the Cygnus Loop will be important test cases for such models in the future.

This work was supported by NASA contract NAS5-32985 to the Johns Hopkins University.

#### REFERENCES

- Blair, W. P., et al. 1991a, *ApJ*, 379, L33
- Blair, W. P., Long, K. S., Vancura, O., & Holberg, J. B. 1991b, *ApJ*, 374, 202
- Blair, W. P., Sankrit, R., Raymond, J. C., & Long, K. S. 1999, *AJ*, 118, 942
- Blair, W. P., Sankrit, R., & Tulin, S. 2002, *ApJS*, 140, 367
- Hester, J. J., Raymond, J. C., & Blair, W. P. 1994, *ApJ*, 420, 721
- Ku, W. H-M., Kahn, S. M., Pisarski, R., & Long, K. S. 1984, *ApJ*, 278, 615
- Levenson, N. A., Graham, J. R., Keller, L. D., Richter, M. J. 1998, *ApJS*, 118, 541
- Long, K. S., et al. 1992, *ApJ*, 400, 214
- Rasmussen, A., & Martin, C. 1992, *ApJ*, 396, L103
- Raymond, J. C. 2003, *RevMexAA(SC)*, 15, 258 (this volume)
- Sankrit, R., Blair, W. P., Raymond, J. C., & Long, K. S. 2000, *AJ*, 120, 1925
- Sankrit, R., & Blair, W. P. 2002, *ApJ*, 565, 297
- Vancura, O., et al. 1993 *ApJ*, 417, 663

William P. Blair and Ravi Sankrit: Rm 144, Bloomberg, The Johns Hopkins University, 3400, N. Charles St., Baltimore, MD 21218, USA (wpb, ravi@pha.jhu.edu).